

Supporting Information

Iron-assisted engineering of molybdenum phosphide nanowires on carbon cloth for efficient hydrogen evolution at a wide pH range

Yuan Teng, Xu-Dong Wang, Hong-Yan Chen,* Jin-Feng Liao, Wen-Guang Li, and Dai-Bin Kuang*

MOE Key Laboratory of Bioinorganic and Synthetic Chemistry, Lehn Institute of Functional Materials, School of Chemistry, Sun Yat-sen University, Guangzhou 510275, P. R. China. Tel: (+86) 20-8411 4399.

*E-mail: chenhy33@mail.sysu.edu.cn; kuangdb@mail.sysu.edu.cn

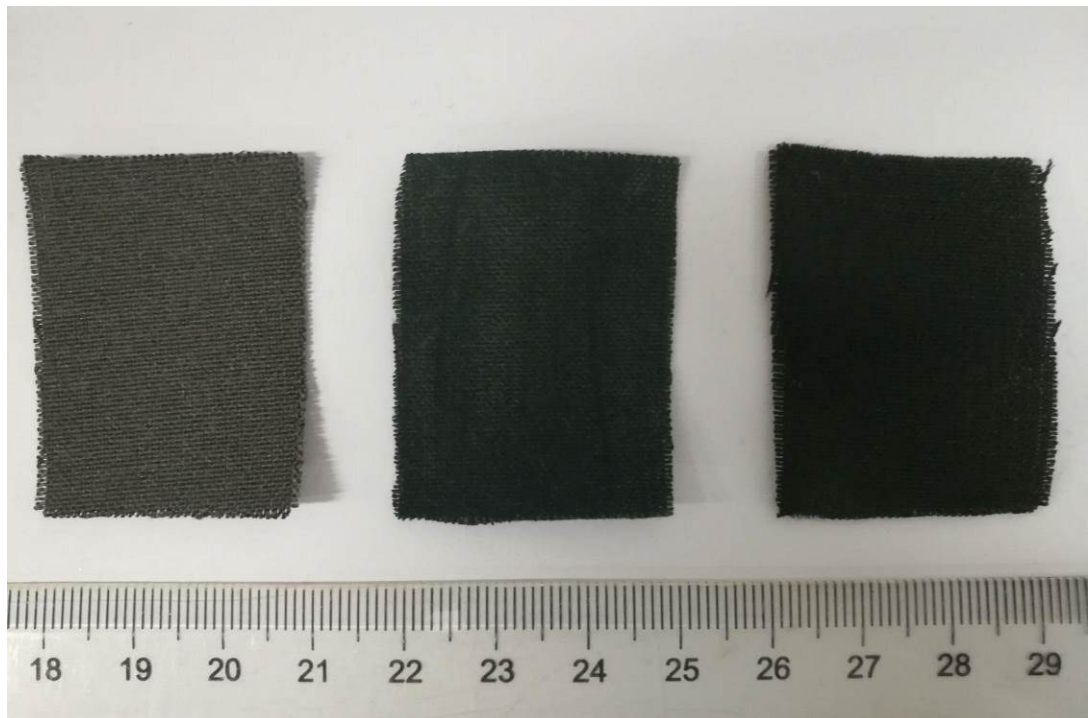


Fig. S1 Photographs of blank carbon cloth (left), Fe-Mo-O/CC precursor (middle), and MoP NWs/CC sample (right).

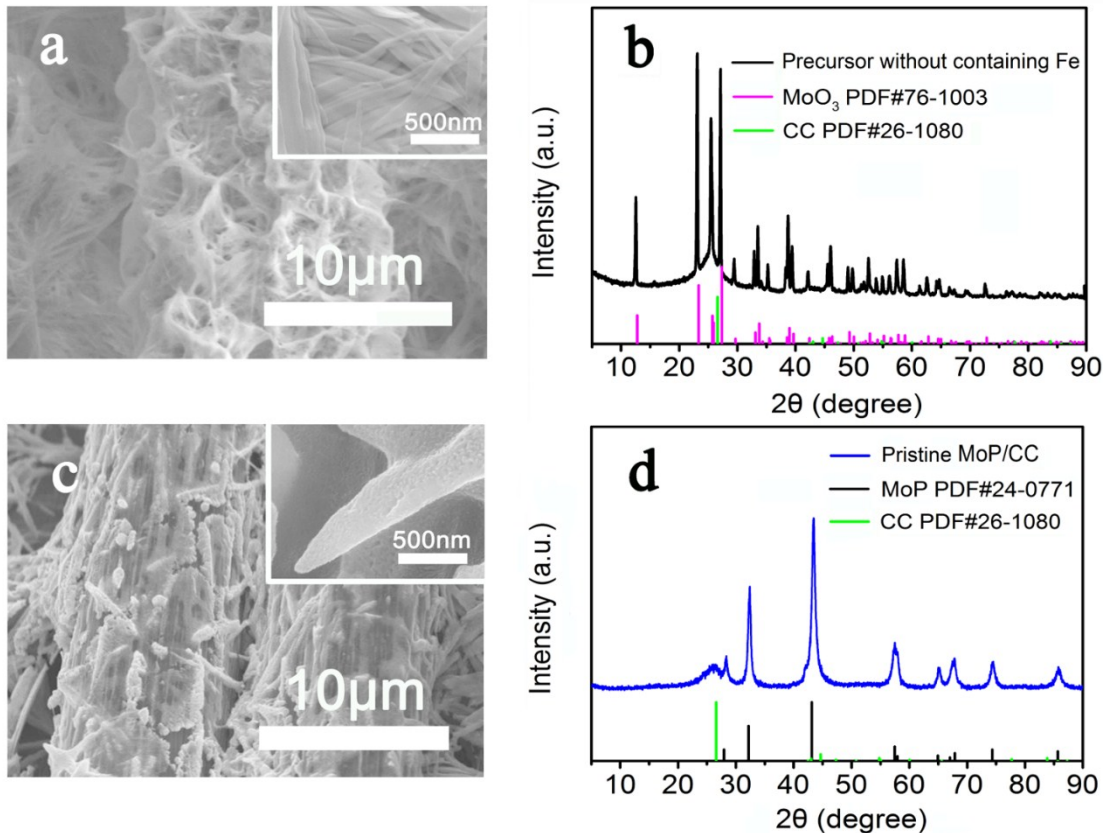


Fig. S2 SEM images and XRD patterns of MoO₃ precursor prepared without the Fe (a, b) and the corresponding pristine MoP/CC (c, d).

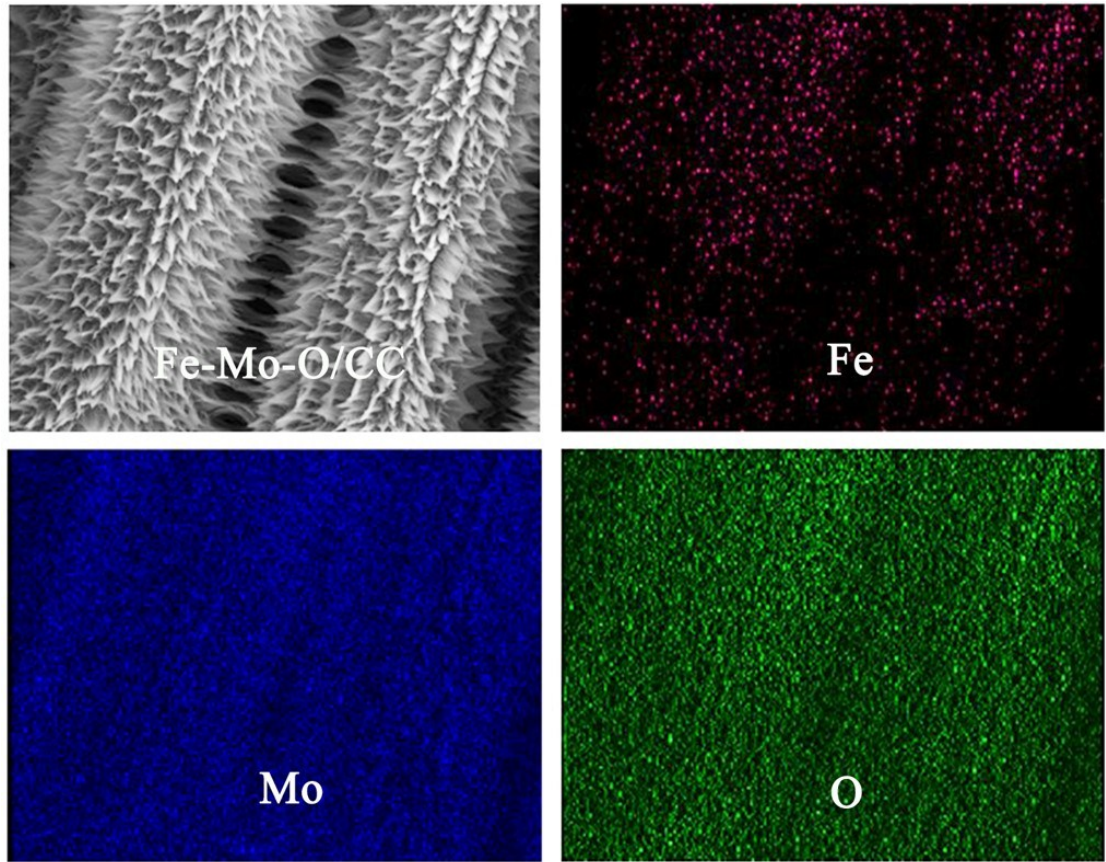


Fig. S3 EDX elemental mapping images of Fe, Mo and O for Fe-Mo-O/CC precursor. It confirms the even distribution of Fe, Mo and O elements in precursor.

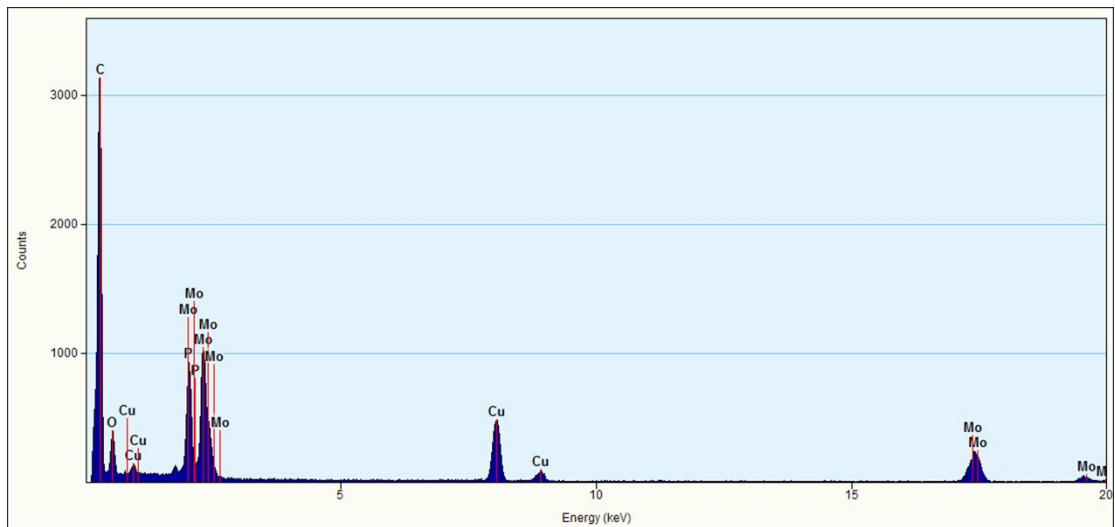


Fig. S4 EDX spectrum for the MoP NWs/CC.

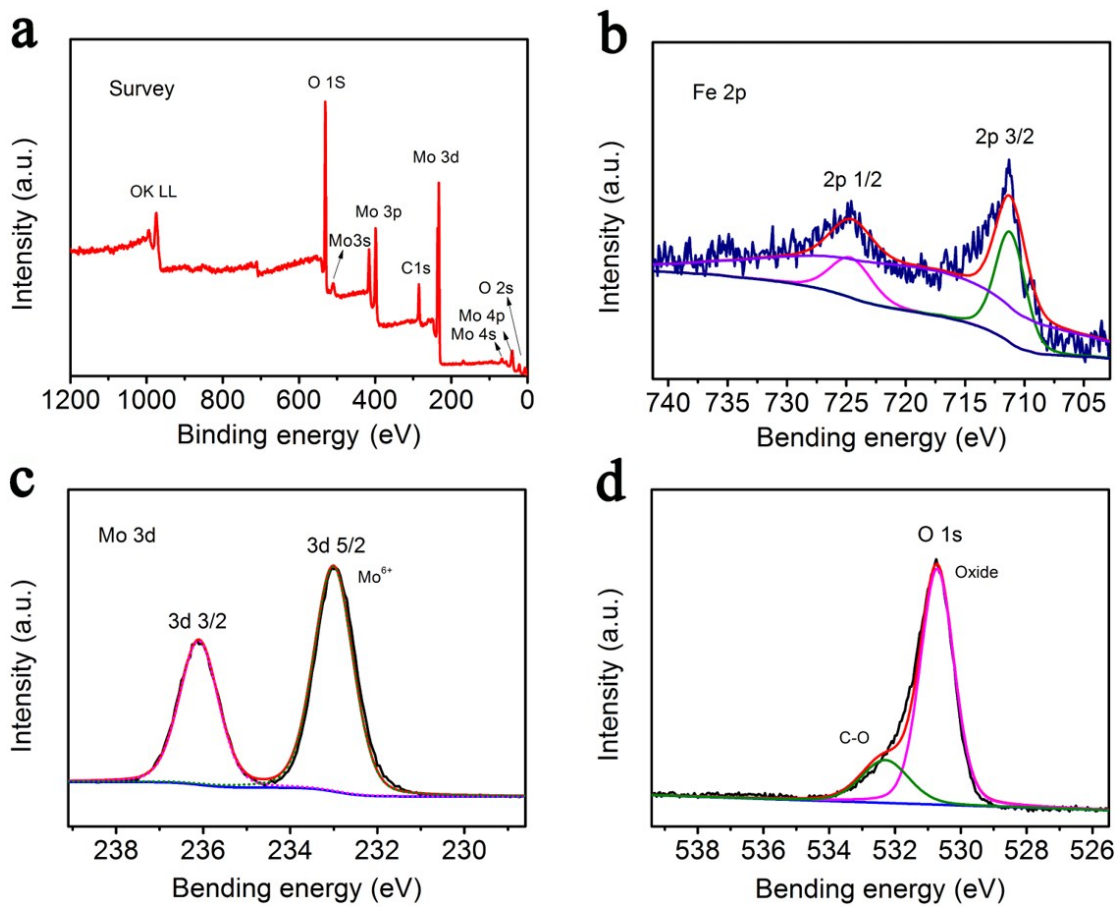


Fig. S5 XPS pattern of Fe-Mo-O/CC: (a) The survey spectrum shows the presence of Mo, Fe, O, and C element on the surface of sample; (b) Fe 2p spectrum which exhibits two peaks at 711.4 eV and 724.7 eV, respectively, displays the type characteristics of Fe^{3+} ; (c) two intense peaks for Mo 3d at 233.2 eV and 236.3 eV correspond to Mo^{6+} , which can belong to MoO_3 ; (d) O 1s region which also presents two peaks at 530.6 eV and 532.3 eV reflects two kinds of oxygen chemical states assigning to the O^{2-} ions in oxide and C-O bonds, respectively.

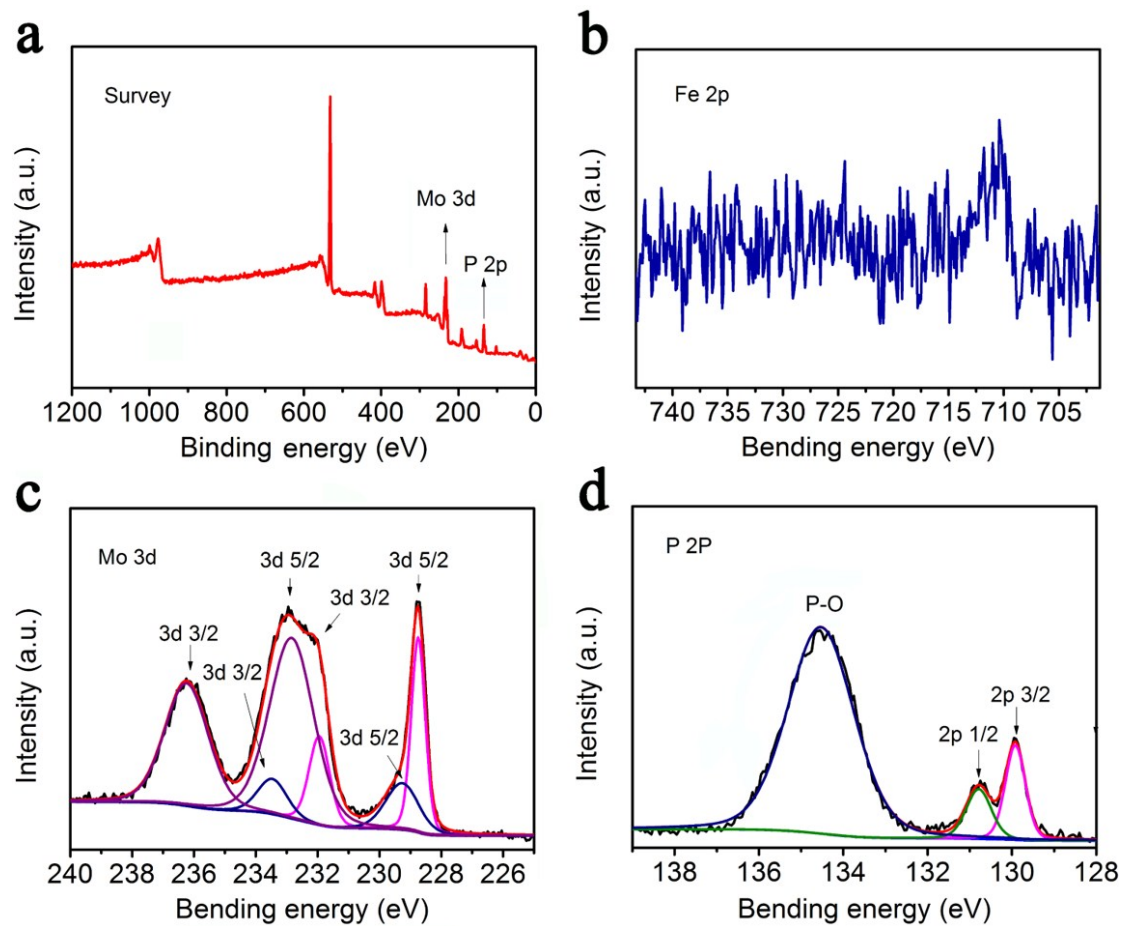


Fig. S6 (a) XPS survey spectrum of the MoP NWs/CC before acid treatment; (b) Fe 2p; (c) Mo 3d; (d) P 2p regions for the MoP NWs/CC before acid treatment: Fe 2p region shows the existence of Fe at high valence; the Mo 3d region, except for the peaks of MoP, also exhibits others peaks that can be attributed to high valence Mo species arising from the further surface oxidation and some residual MoO₂; for P 2p region, large packet peak at high bending energy belongs to P-O species that are also due to superficial oxidation, and P 2p region can be assigned to P into phosphide.

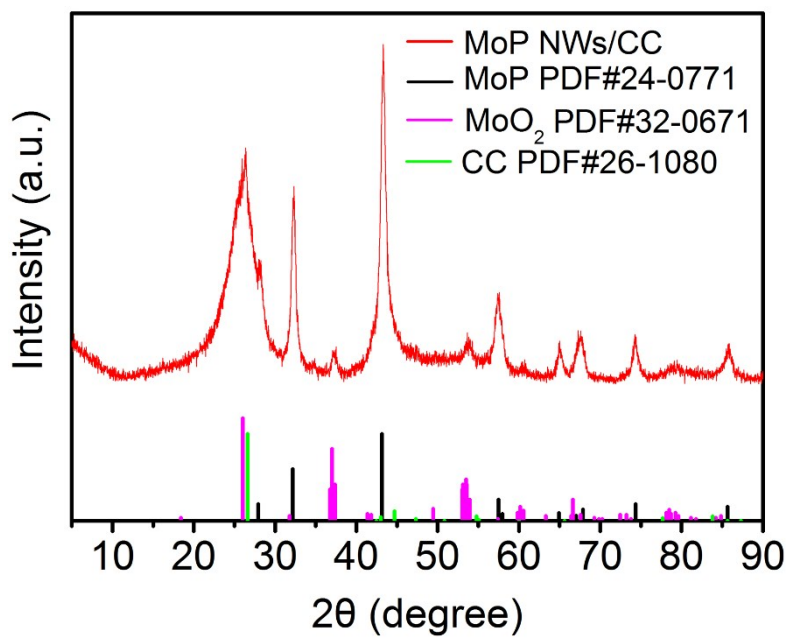


Fig. S7 XRD pattern of the MoP NWs/CC before acid treatment, which shows small peaks indexed to MoO₂ residual.

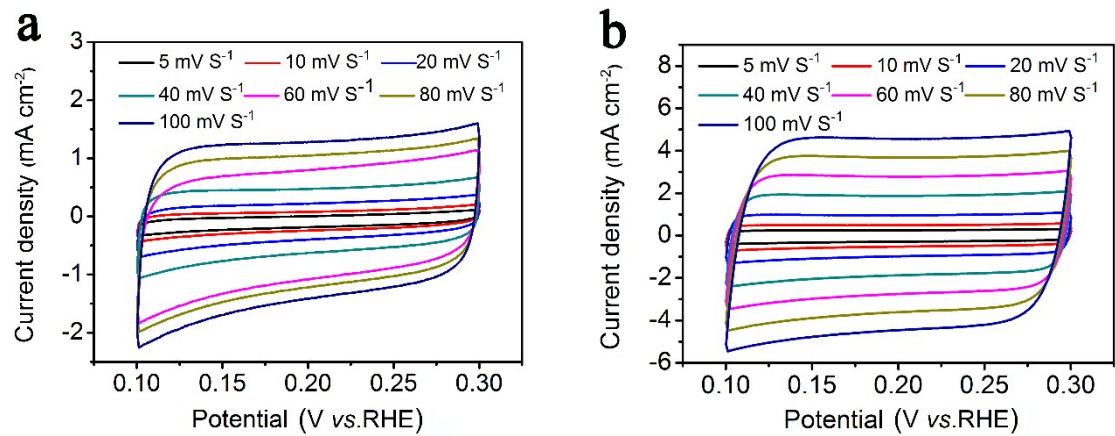


Fig. S8 Cyclic voltammograms in the region of 0.1-0.3 V *vs.* RHE at various scan rates of (a) pristine MoP/CC and (b) MoP NWs/CC.

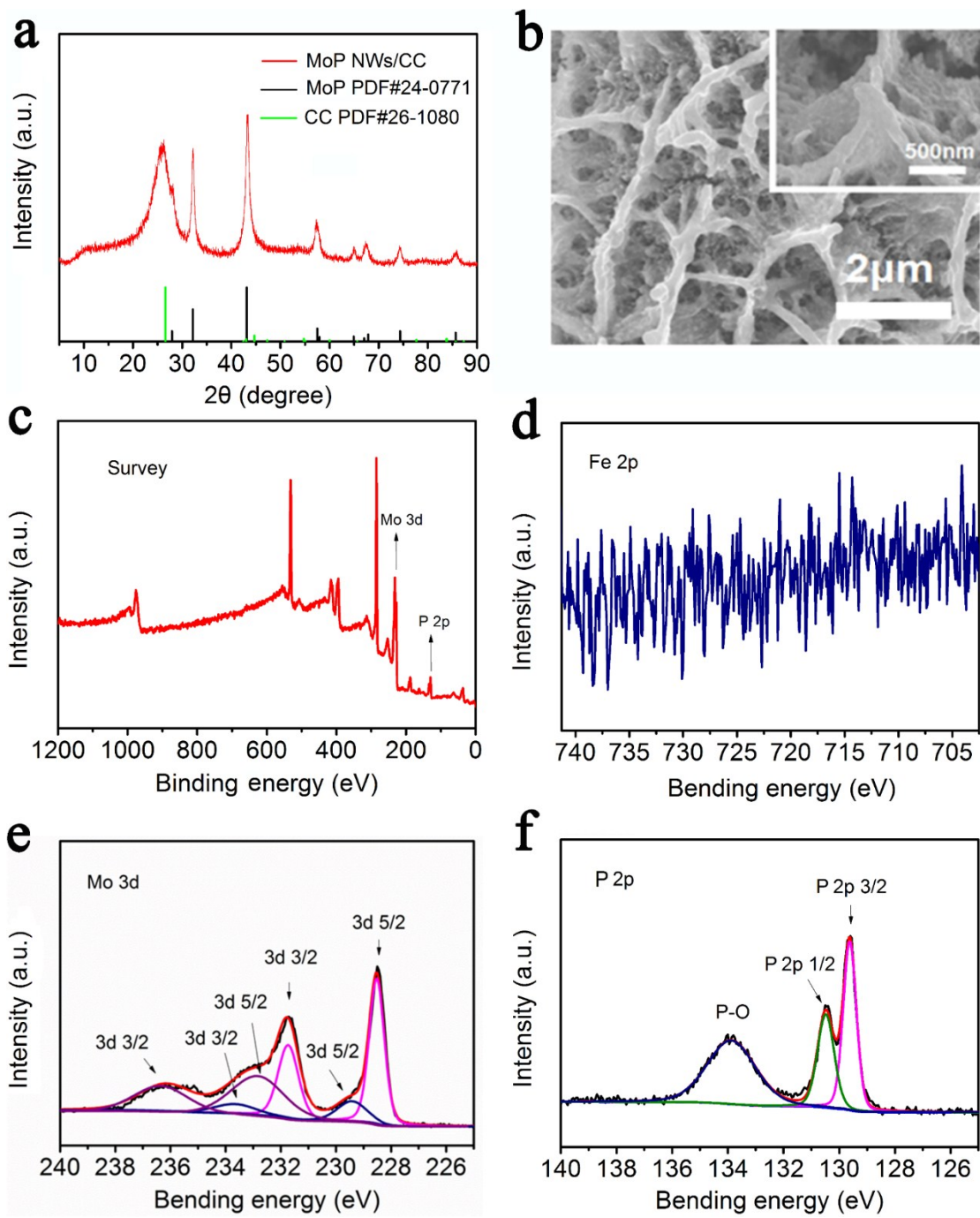


Fig. S9 Structure and composition characterization of the MoP NWs/CC after a 24 h stability test: (a) XRD pattern presents a pure MoP phase; (b) the SEM images after stability tests doesn't appear to induce obvious morphological changes; (c-f) XPS spectrum after the stability tests indicates the well-maintained surface chemical state.

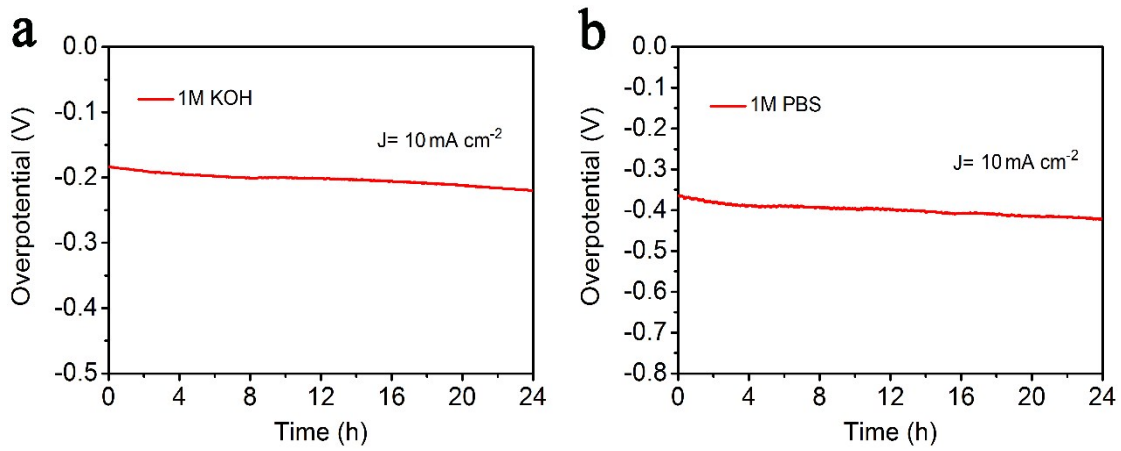


Fig. S10 Chronopotentiometric curves for the CV-processed MoP NWs/CC at a static current density of 10 mA cm^{-2} for 24 h in 1 M KOH (a) and 1 M PBS (b) electrolytes, respectively.

Table S1 Comparison of HER performance in acid electrolytes for HER electrocatalysts in the literatures and this work

Catalysts	Loading mass (mg cm ⁻²)	Tafel slope (mV dec ⁻¹) ¹⁾	Current density (<i>j</i> , mA cm ⁻²) ²⁾	Overpotential at the corresponding <i>j</i> (mV)	Exchange current density (<i>j</i> , mA cm ⁻²)	Ref.
MoP	0.071	60	10	246	0.004	1
MoP-CA ₂	0.36	54	10/100	125/200	0.086	2
Commercial MoP	~0.1	50	10	150	0.01	3
MoP	~1	50	10/100	117/180	0.05	4
MoP S	~3	50	10/100	64/120	0.57	4
Mo-W-P	4.0	52	20/100	93/138	-	16
MoP ₂	1	52	10/100	121/193	-	5
Fe-promoted MoP	0.071	49	10	195	-	6
Pristine MoP/CC	2	60.8	10/100	173/241	0.014	This work
MoP NWs/CC	2	53.3	10/100	113/174	0.075	This work

Table S2 Comparison of HER performance in alkaline electrolytes for HER electrocatalysts in the literatures and this work

Catalysts	Loading mass (mg cm ⁻²)	Tafel slope (mV dec ⁻¹)	Current density (j , mA cm ⁻²)	Overpotential at the corresponding j (mV)	Exchange current density (j , mA cm ⁻²)	Ref.
CoP/CC	0.92	129	10	209	-	7
FeP/CC	1.5	146	10	218	-	8
WP/CC	2	102	10	150	-	9
MoB	2.3	59	5	250	0.002	10
MoC _x	0.8	59	10	151	0.029	11
Mo ₂ C-NCNT	~3	-	10	257	-	12
Ni	-	-	10	400	-	10
Co-S/FTO	0.0796	-	1	480	-	15
Amorphous MoS ₂ /FTO	-	-	10	540	-	17
Ni wire	-	-	10	350	-	18
Pristine MoP/CC	2	86.1	10/100	231/332	0.021	This work
MoP NWs/CC	2	65.6	10/100	103/181	0.279	This work

Table S3 Comparison of HER performance in neutral electrolytes for HER electrocatalysts in the literatures and this work

Catalysts	Loading mass (mg cm ⁻²)	Tafel slope (mV dec ⁻¹)	Current density (j , mA cm ⁻²)	Overpotential at the corresponding j (mV)	Exchange current density (j , mA cm ⁻²)	Ref.
Co-NRCNTs	~0.28	-	2/10	380/540	-	13
Mo ₂ B	2.3	-	1	250	-	10
Mo ₂ C	-	-	1	200	-	10
H ₂ -CoCat/FTO	-	140	2	385	-	14
CuMoS ₄ crystals	0.0416	95	2	210	-	19
Pristine MoP/CC	2	147.8	2/10	289/412	0.016	This work
MoP NWs/CC	2	119.4	2/10	63/232	0.114	This work

References

- 1 X. B. Chen, D. Z. Wang, Z. P. Wang, P. Zhou, Z. Z. Wu, F. Jiang, *Chem. Commun.*, 2014, **50**, 11683-11685.
- 2 Z. C. Xing, Q. Liu, A. M. Asiri, X. P. Sun, *Adv. Mater.*, 2014, **26**, 5702-5707.
- 3 T. Y. Wang, K. Z. Du, W. L. Liu, Z. W. Zhu, Y. H. Shao, M. X. Li, *J. Mater. Chem. A*, 2015, **3**, 4368-4373.
- 4 J. Kibsgaard, T. F. Jaramillo, *Angew. Chem. Int. Ed.*, 2014, **53**, 14433-14437.
- 5 T. L. Wu, M. Y. Pi, D. K. Zhang, S. J. Chen, *J. Power Sources*, 2016, **328**, 551-557.
- 6 X. Liang, D. Z. Zhang, Z. Z. Wu, D. Z. Wang, *Appl. Catal. A: Gen.*, 2016, **524**, 134-138.
- 7 J. Q. Tian, Q. Liu, A. M. Asiri, X. P. Sun, *J. Am. Chem. Soc.*, 2014, **136**, 7587-7590.
- 8 Y. H. Liang, Q. Liu, A. M. Asiri, X. P. Sun, Y. L. Luo, *ACS Catal.*, 2014, **4**, 4065-4069.
- 9 Z. H. Pu, Q. Liu, A. M. Asiri, X. P. Sun, *ACS Appl. Mater. Interfaces*, 2014, **6**, 21874-21879.
- 10 H. Vrubel, X. L. Hu, *Angew. Chem. Int. Ed.*, 2012, **51**, 12703-12706.
- 11 H. B. Wu, B. Y. Xia, L. Yu, X.-Y. Yu, X. W. Lou, *Nat. Chem.*, 2015, **6**, 6512.
- 12 K. Zhang, Y. Zhao, D. Y. Fu, Y. J. Chen, *J. Mater. Chem. A*, 2015, **3**, 5783-5788.
- 13 X. X. Zou, X. X. Huang, A. Goswami, R. Silva, B. R. Sathe, E. Mikmeková, T. Asefa, *Angew. Chem. Int. Ed.*, 2014, **53**, 4372-4376.
- 14 S. Cobo, J. Heidkamp, P.-A. Jacques, J. Fize, V. Fourmond, L. Guetaz, B. Jousselme, V. Ivanova, H. Dau, S. Palacin, M. Fontecave, V. Artero, *Nat. Mater.*, 2012, **11**, 802-807.
- 15 Y. J. Sun, C. Liu, D. C. Grauer, J. Yano, J. R. Long, P. D. Yang, C. J. Chang, *J. Am. Chem. Soc.*, 2013, **135**, 17699-17702.
- 16 X. D. Wang, Y. F. Xu, H. S. Rao, W. J. Xu, H. Y. Chen, W. X. Zhang, D. B. Kuang and C. Y. Su, *Energy Environ. Sci.*, 2016, **9**, 1468-1475.
- 17 D. Merki, S. Fierro, H. Vrubel and X. L. Hu, *Chem. Sci.*, 2011, **2**, 1262-1267.
- 18 J. R. McKone, B. F. Sadtler, C. A. Werlang, N. S. Lewis, H. B. Gray, *ACS Catal.*, 2013, **3**, 166-169.
- 19 P. D. Tran, M. Nguyen, S. S. Pramana, A. Bhattacharjee, S. Y. Chiam, J. Fize, M. J. Field, V. Artero, L. H. Wong, J. Loo and J. Barber, *Energy Environ. Sci.* 2012, **5**, 8912-8916.

Supplementary Movie

This video exhibits as-synthesized MoP NWs/CC electrode operated at a large current density of 80 mA cm⁻² to drive hydrogen evolution reaction in 0.5 M H₂SO₄ solution. Substantial hydrogen bubbles are generated and quickly released from the electrodes.